Advancements in DOI-capable TOF-PET modules based on High-Frequency Readout

Giulia Terragni [1 2], Elena Tribbia [1 3], Carsten Lowis [1 4], Fiammetta Pagano [1 3 5],
Joshua W. Cates [6], Marco Pizzichemi [1 3], Johann Marton [2], Etiennette Auffray [1]

[1] CERN, Geneva, Switzerland. [2] Technical University of Vienna, Austria.
[3] University of Milano-Bicocca, Italy. [4] RWTH Aachen University, Germany.
[5] Institute of Instrumentation for Molecular Imaging (I3M), Valencia, Spain.
[6] Lawrence Berkeley National Laboratory, CA, USA.

28th May 2024
PM2024 - 16th Pisa Meeting on Advanced Detectors

TOF-PET

Fundamental requirements

To obtain as many counts as possible:

- High **sensitivity**

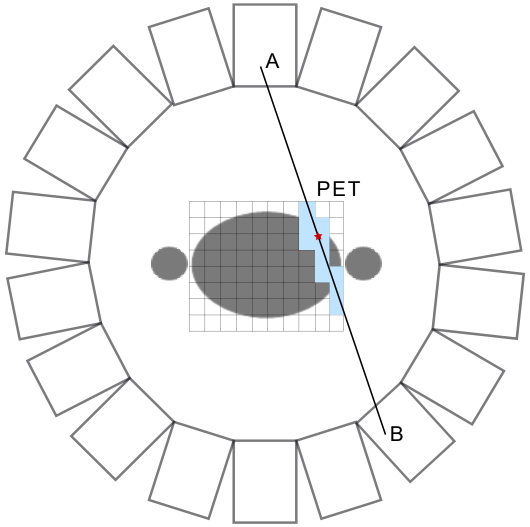

Long scintillator maximize sensitivity
But
Parallax effect degrades the spatial resolution

To characterize them as accurate as possible:

- High **spatial resolution**
- High **timing resolution**
- High **energy resolution**

TOF-PET

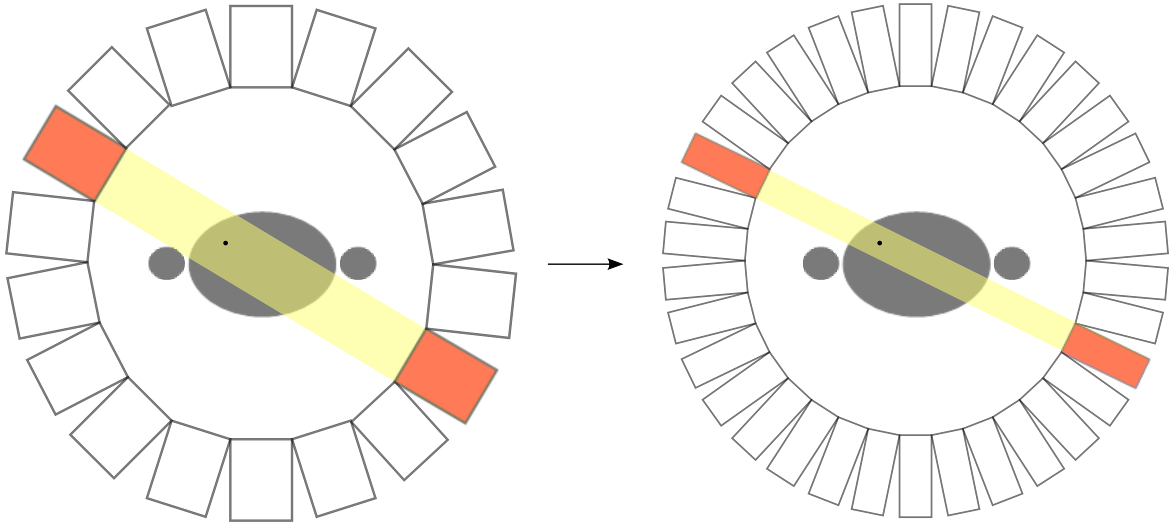

Fundamental requirements

To obtain as many counts as possible:

- High **sensitivity**

Long scintillator maximize sensitivity
But
Parallax effect degrades the spatial resolution

To characterize them as accurate as possible:

- High **spatial resolution**

Segmentation improves spatial resolution

- High **timing resolution**

- High **energy resolution**

TOF-PET

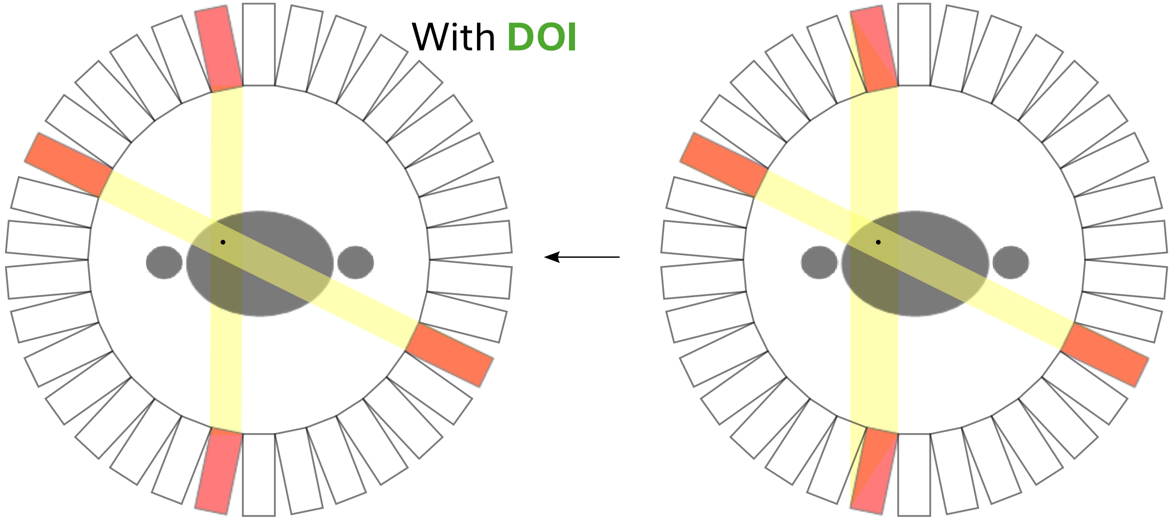

Fundamental requirements

To obtain as many counts as possible:

- High **sensitivity**

Long scintillator maximize sensitivity
But
Parallax effect degrades the spatial resolution

To characterize them as accurate as possible:

- High **spatial resolution**

Segmentation improves spatial resolution
And
Recovering resolution is possible if the **depth of interaction (DOI)** of the gamma rays is measured

- High **timing resolution**

- High **energy resolution**

TOF-PET

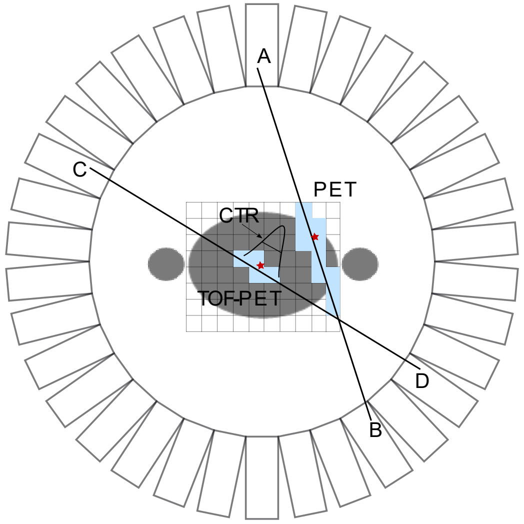

Fundamental requirements

To obtain as many counts as possible:

- High **sensitivity** → **Long scintillator** maximize sensitivity **But** **Parallax effect** degrades the spatial resolution

To characterize them as accurate as possible:

- High **spatial resolution** → **Segmentation** improves spatial resolution **And** Recovering resolution is possible if the **depth of interaction (DOI)** of the gamma rays is measured
- High **timing resolution** → Improve **event localization** along the line of response (LOR) **And** Improve **signal-to-noise ratio** (SNR)
- High **energy resolution**

TOF-PET

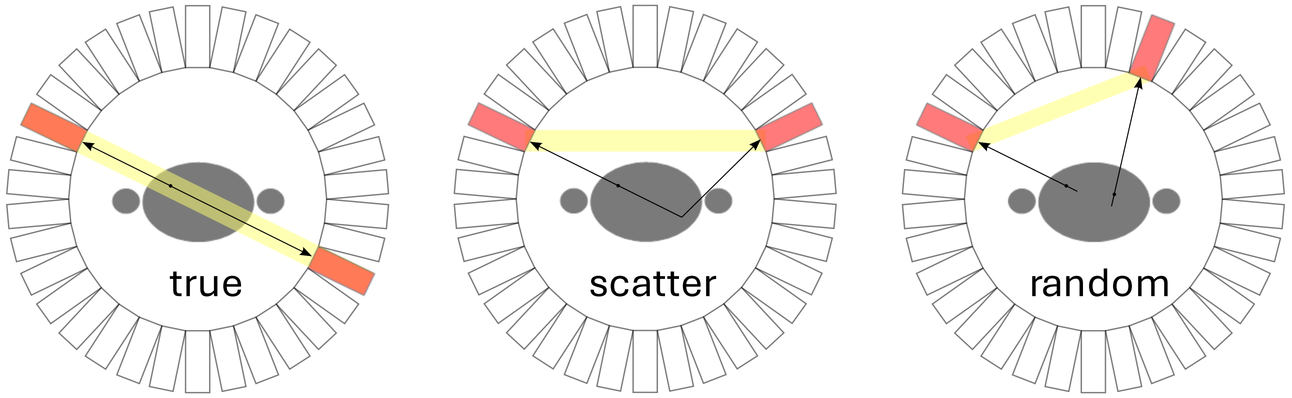

Fundamental requirements

To obtain as many counts as possible:

- High **sensitivity** → **Long scintillator** maximize sensitivity **But** **Parallax effect** degrades the spatial resolution

To characterize them as accurate as possible:

- High **spatial resolution** → **Segmentation** improves spatial resolution **And** Recovering resolution is possible if the **depth of interaction (DOI)** of the gamma rays is measured
- High **timing resolution** → Improve **event localization** along the line of response (LOR) **And** Improve **signal-to-noise ratio** (SNR)
- High **energy resolution** → Improve **signal discrimination**

TOF-PET

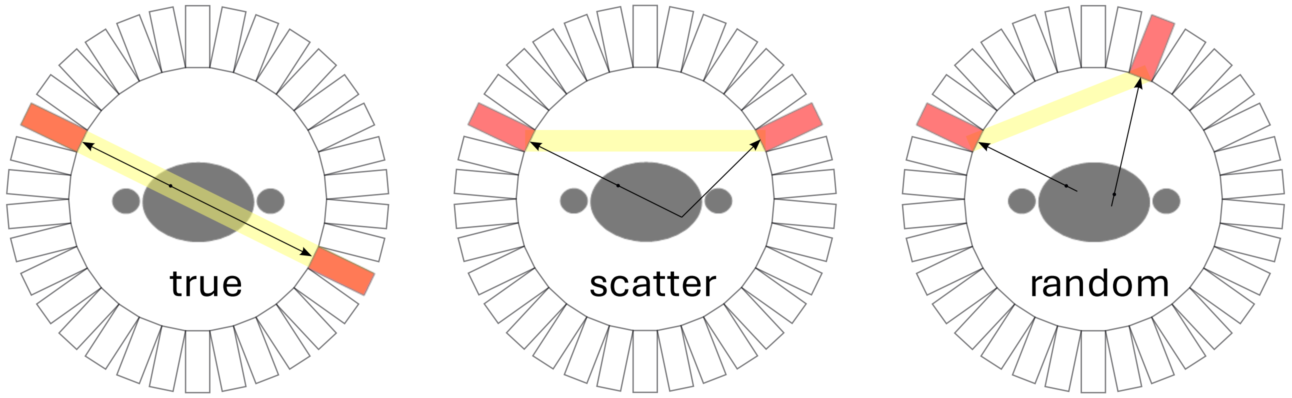

Fundamental requirements

To obtain as many counts as possible:

- High **sensitivity** → **Long scintillator** maximize sensitivity **But** **Parallax effect** degrades the spatial resolution

To characterize them as accurate as possible:

- High **spatial resolution** → **Segmentation** improves spatial resolution **And** Recovering resolution is possible if the **depth of interaction (DOI)** of the gamma rays is measured
- High **timing resolution** → Improve **event localization** along the line of response (LOR) **And** Improve **signal-to-noise ratio** (SNR)
- High **energy resolution** → Improve **signal discrimination**

Segmented DOI-capable TOF-PET Module

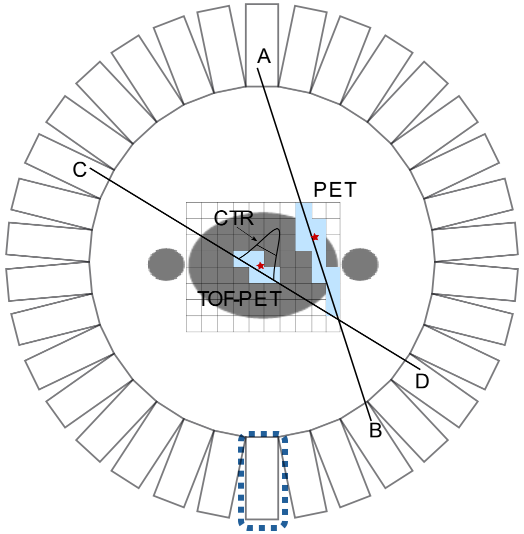

- Segmented matrix of 4x4 crystals from Crystal Photonics Inc (CPI)
- Coupled to an array of 4x4 Silicon Photomultiplier (SiPM) Broadcom NUV-MT

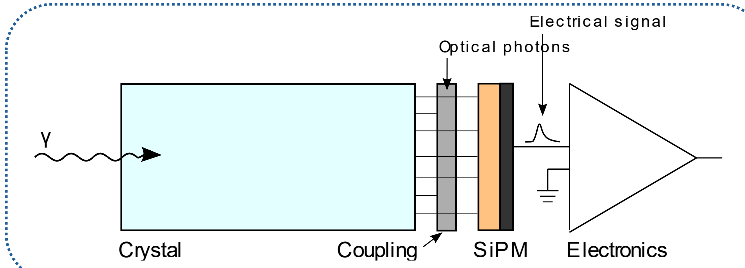

DOI-capable module

Depolished crystals lateral surfaces, with a light-guide and a reflector on top [1]

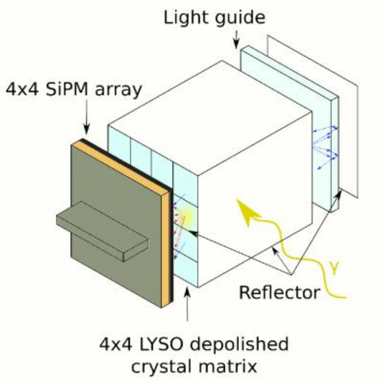

Standard module

Polished crystals with a reflector on top

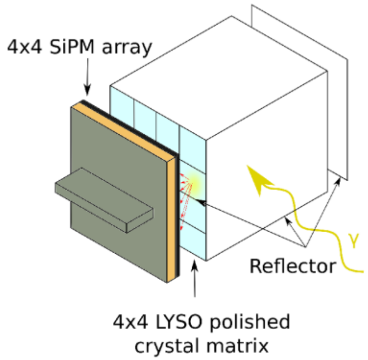

[1] *M. Pizzichemi et al. Physics in Medicine & Biology, 2016, 61.12: 4679.*

Segmented DOI-capable TOF-PET Module

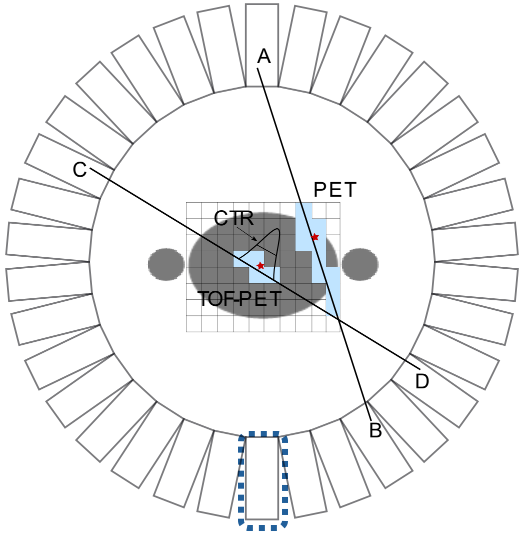

- Segmented matrix of 4x4 crystals from Crystal Photonics Inc (CPI)
- Coupled to an array of 4x4 Silicon Photomultiplier (SiPM) Broadcom NUV-MT

DOI-capable module

Depolished crystals lateral surfaces, with a light-guide and a reflector on top [1]

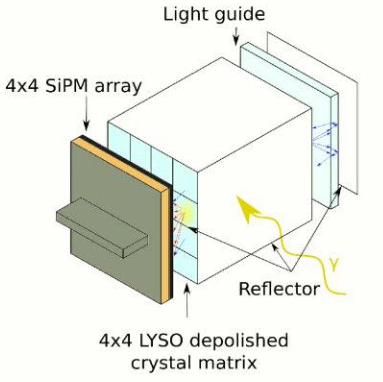

Energy:

$$P = \sum_{i=1}^{K} p_i.$$

Coordinates of gammas interaction point:

$$u = \frac{1}{P}\sum_{i=1}^{K} p_i x_i \qquad v = \frac{1}{P}\sum_{i=1}^{K} p_i y_i \qquad w = \frac{p_{max}}{P}$$

Time:

$$\Delta t_{std} = t_1 - t_{ref}$$

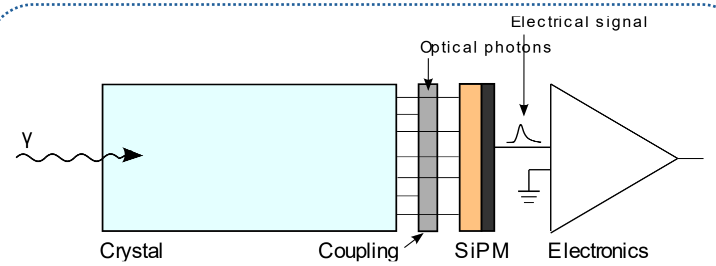

$i = 1$
$p_1 = p_{max}$ SiPM coupled to the crystal where the interaction occurred

[1] *M. Pizzichemi et al. Physics in Medicine & Biology, 2016, 61.12: 4679.*

Development board

Low-Noise Low-Power High-Frequency Multi-Channel development board [2]**:**

- Each SiPM output signal is split and processed by:
  - High-frequency circuit having a **low-noise amplifier** chain and **fast discriminator** to extract a fast-time digital signal. → **Time**
  - **Low-power operational amplifier** to extract an analog energy signal. → **Energy**
- **Global energy output** is used to trigger two CAEN V1742 32-ch digitizers (5 Gs/s, 500 MHz bandwidth) for the digitization of the signals

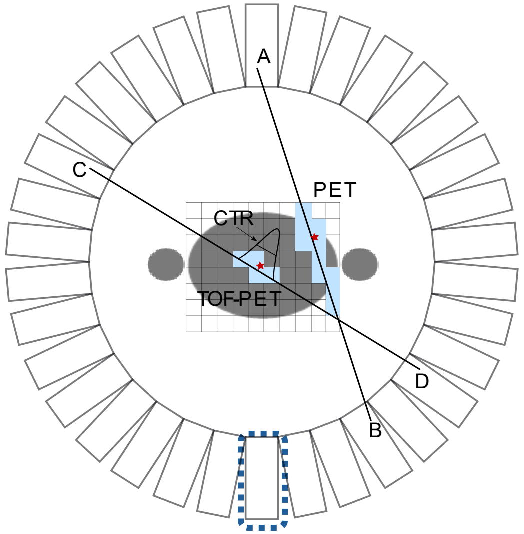

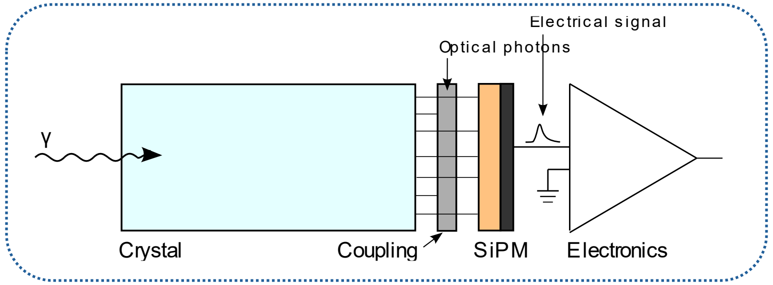

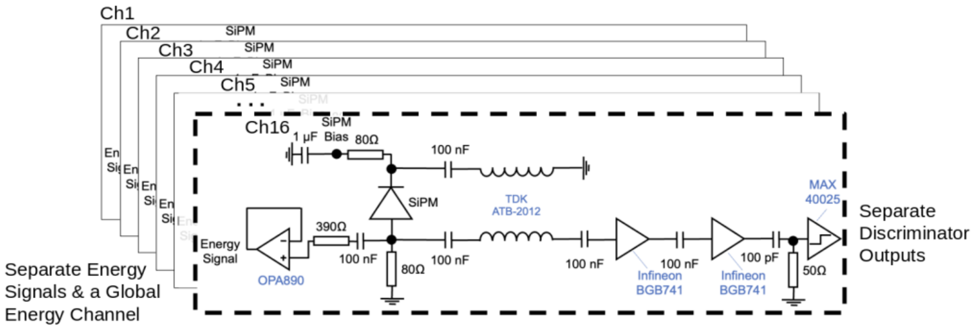

[2] *J. W. Cates and W. S. Choong (2022) Physics in Medicine & Biology, 67 195009.*

Experimental set-up

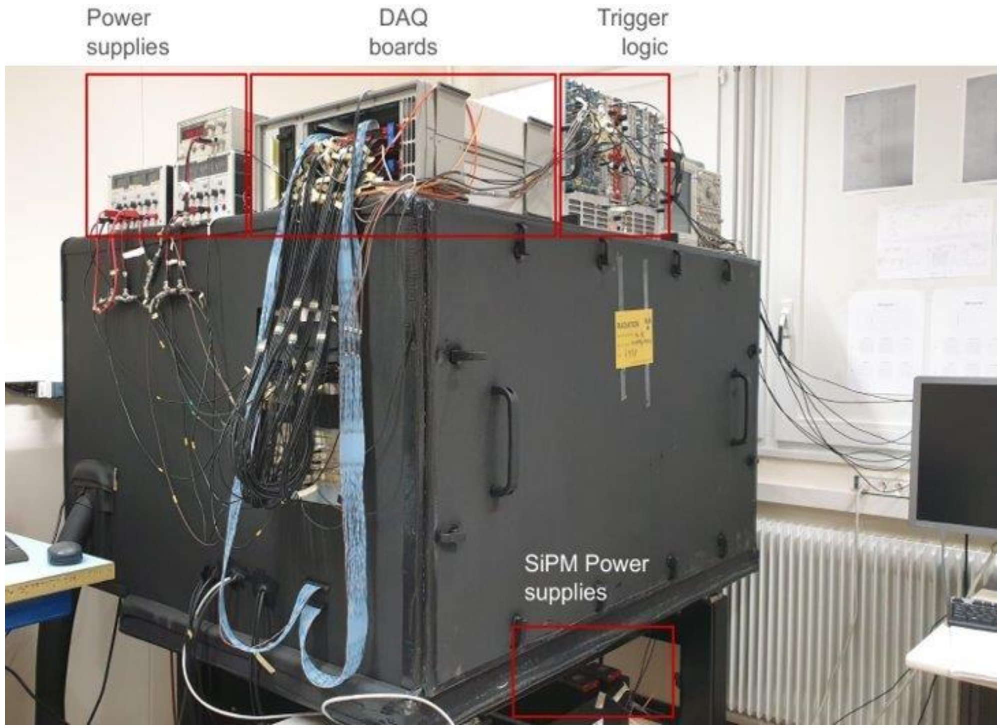

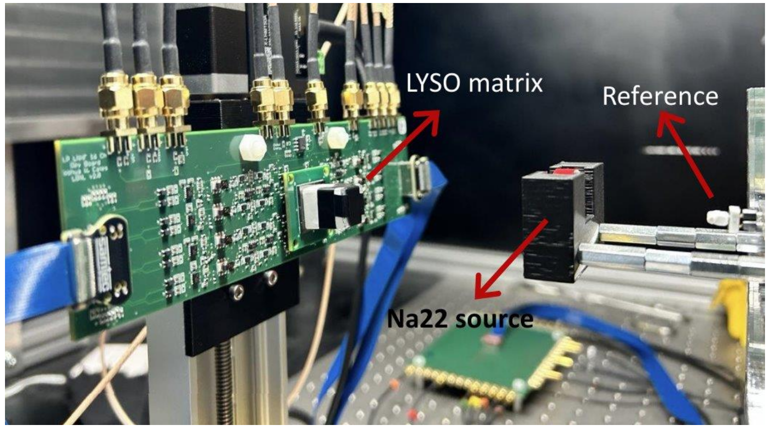

Analysis:

1. SiPM array Saturation correction

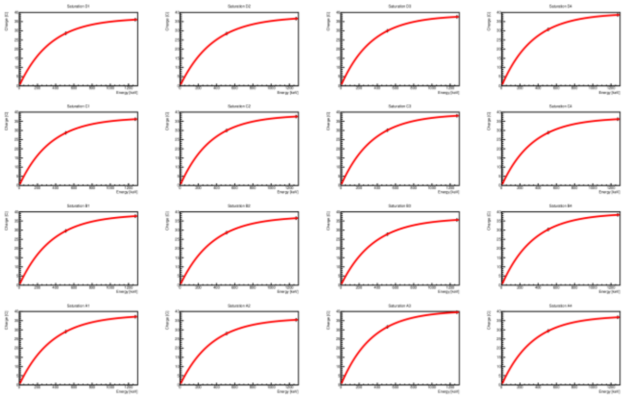

2. Selection of events in the photopeak of the reference crystal

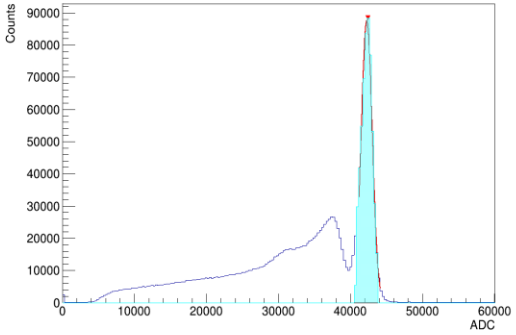

3. Crystal separation and selection of energy deposition in one crystal

$$u = \frac{1}{P}\sum_{k=1}^{K} p_k x_k \ , \quad v = \frac{1}{P}\sum_{i=k}^{K} p_k y_k \ , \quad w = \frac{p_{max}}{P}$$

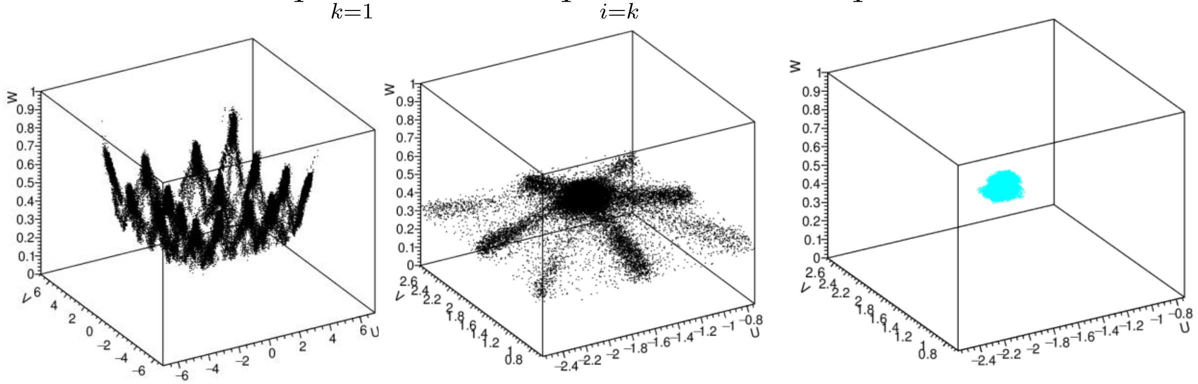

A. Energy selection and **Energy resolution** evaluation for each crystal

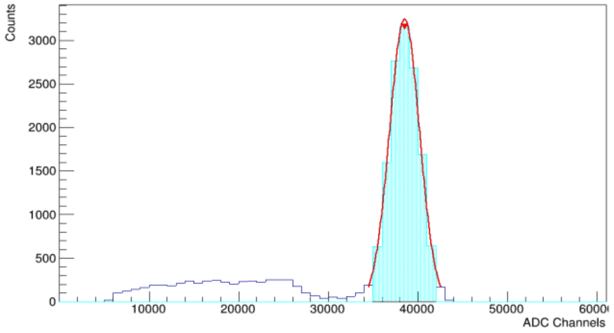

B. **CTR** evaluation for each crystal after correction for the reference

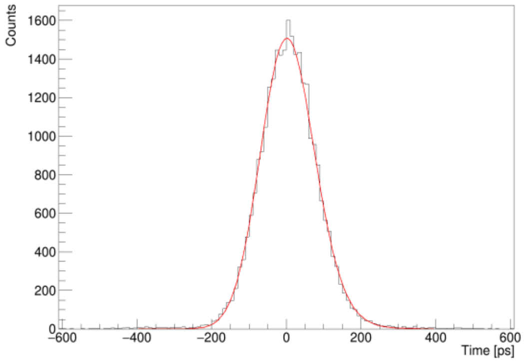

Analysis:

4. DOI calibration [3]

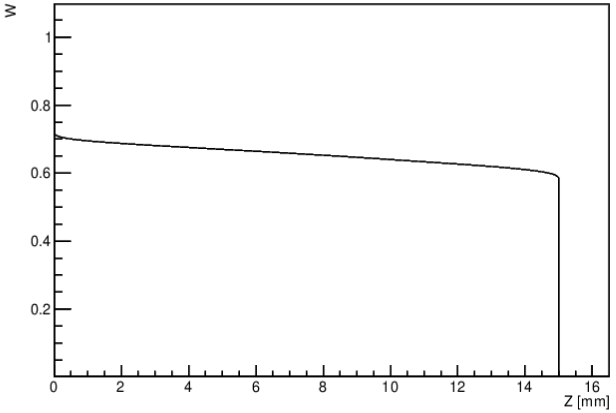

$$\Delta t_{corr} = \hat{\Theta}_{in} - t_{ref}$$

$$\hat{\Theta}_{in} = \frac{\sum_{i=1}^{16}(1/\sigma^2)\cdot(t_i - g_i(w))}{\sum_{i=1}^{16}(1/\sigma^2)} - [d(w) - d(w_0)]$$

5. Timing calibration [4]

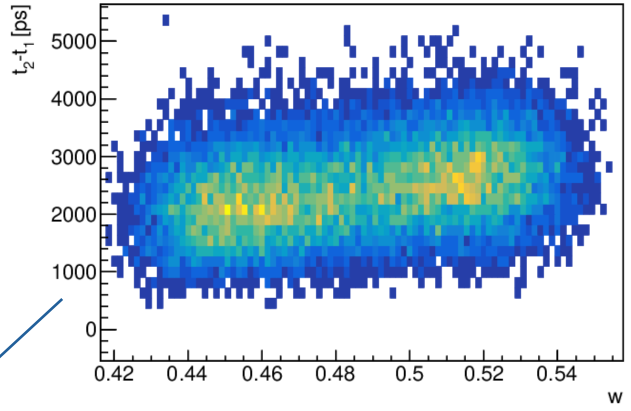

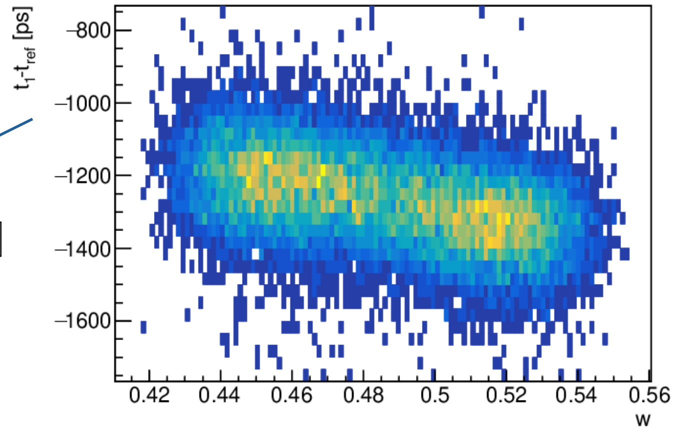

C. **CTR** evaluation for each crystal after correction for the reference

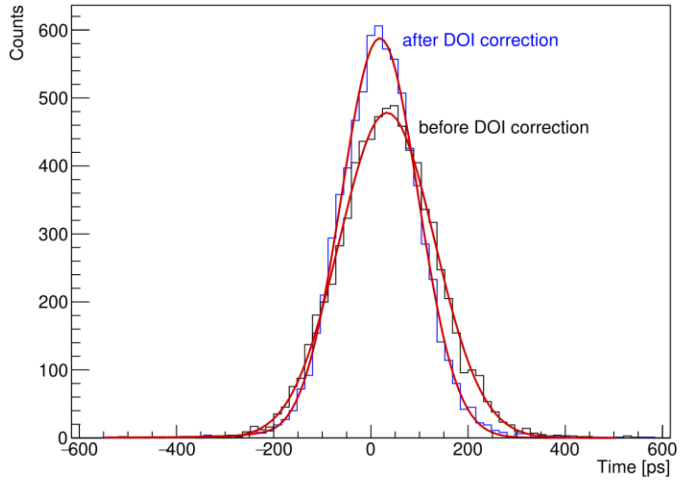

[3] *G. Stringhini et al 2016 DOI 10.1088/1748-0221/11/11/P11014.*
[4] *M. Pizzichemi et al 2019 Phys. Med. Biol. 64 155008.*

Analysis:

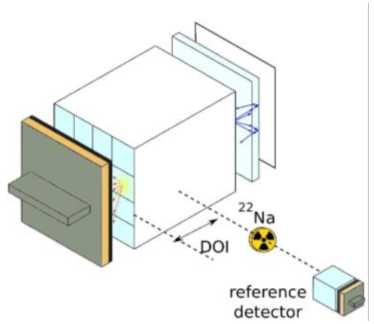

4. DOI calibration [3]

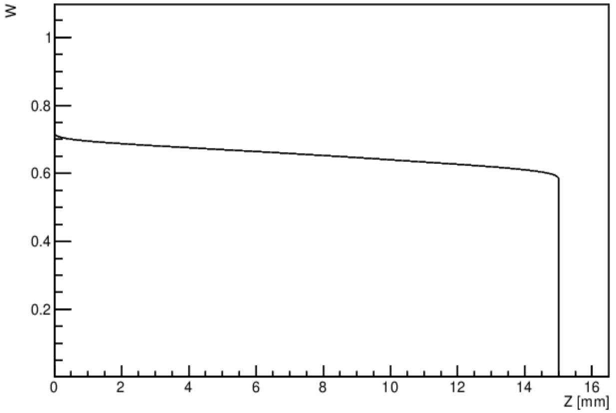

5. Timing calibration [4]

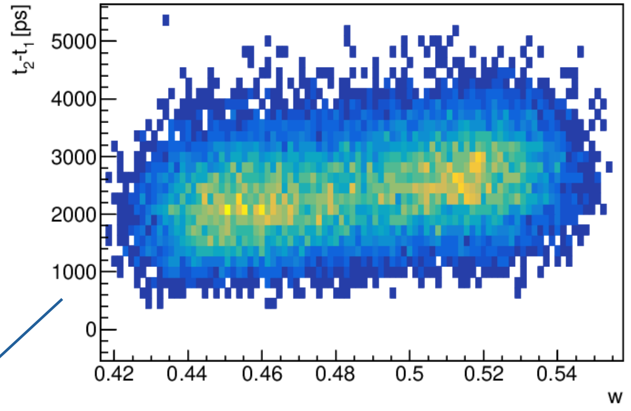

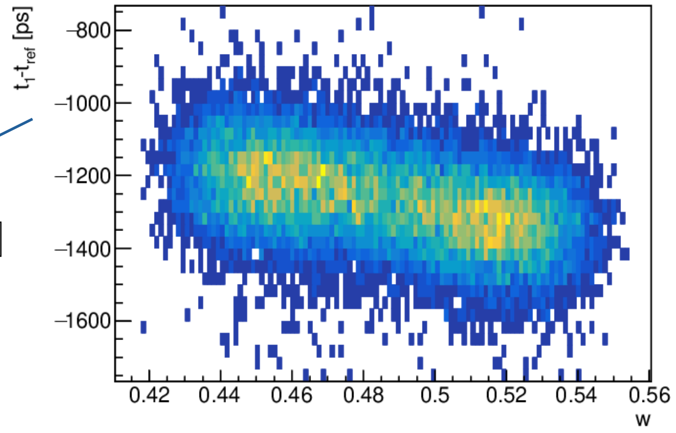

$$\Delta t_{corr} = \hat{\Theta}_{in} - t_{ref}$$

$$\hat{\Theta}_{in} = \frac{\sum_{i=1}^{16}(1/\sigma^2)\cdot(t_i - g_i(w))}{\sum_{i=1}^{16}(1/\sigma^2)} - [d(w) - d(w_0)]$$

D. **DOI resolution** evaluation in lateral irradiation

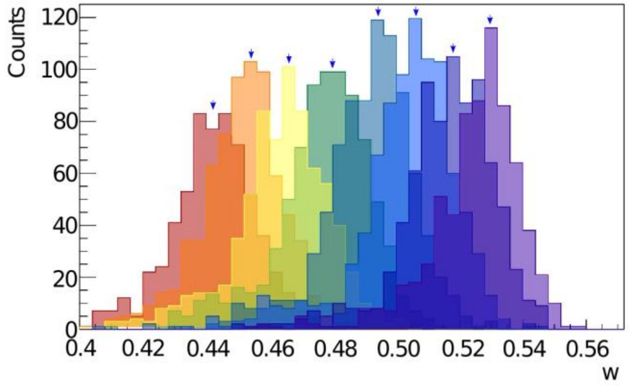

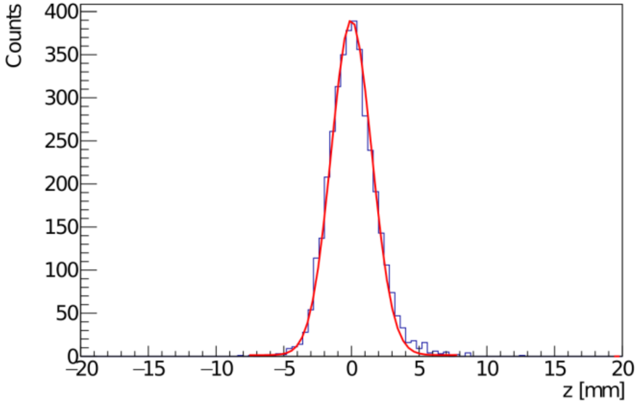

[3] *G. Stringhini et al 2016 DOI 10.1088/1748-0221/11/11/P11014.*
[4] *M. Pizzichemi et al 2019 Phys. Med. Biol. 64 155008.*

LYSO:Ce matrices 3.1x3.1x15 mm^3:

Standard module:

Front irradiation:

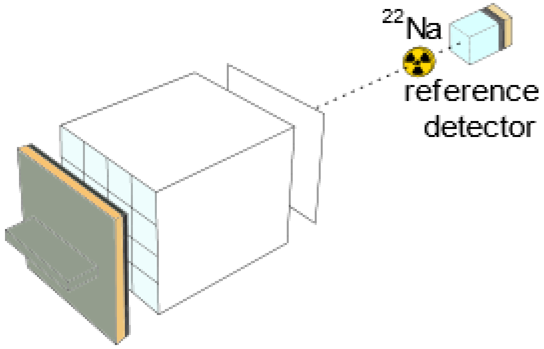

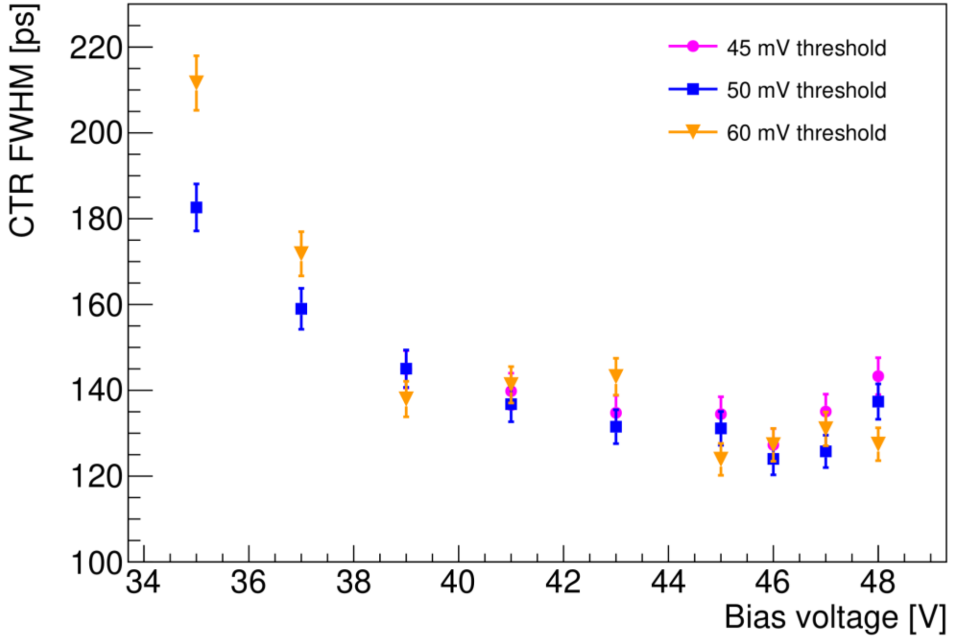

CTR = 124 ± 3 ps FWHM @ 45V and 60 mV

En res = 8.2 ± 0.2 %

LYSO:Ce matrices 3.1x3.1x15 mm^3:

DOI- capable module:

Front irradiation:

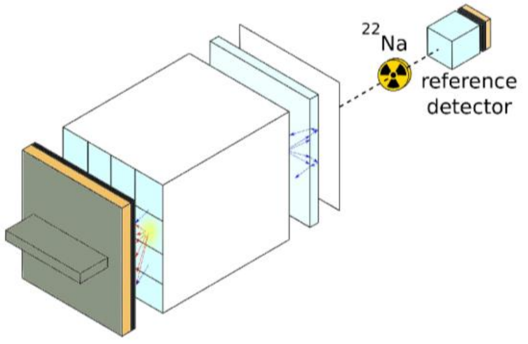

Matrix type	V bias [V]	Thr. [mV]	En. Res FWHM [%]	**CTR std FWHM [ps]**	**CTR doi corr. FWHM [ps]**
DOI-capable	45	60	9.7 ± 0.4	**196 ± 6**	**146 ± 4**
Standard	45	60	8.2 ± 0.2	**124 ± 3**	**-**

LYSO:Ce matrices 3.1x3.1x15 mm^3:

DOI- capable module:

Lateral irradiation:

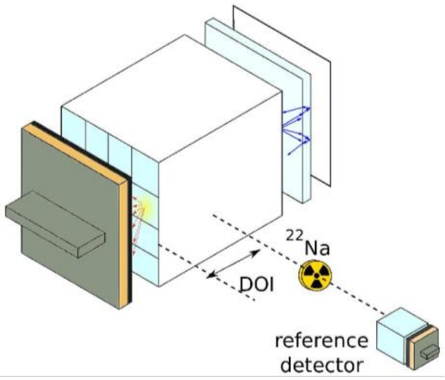

Matrix type	V bias [V]	Thr. [mV]	En. Res FWHM [%]	**CTR std FWHM [ps]**	**CTR doi corr. FWHM [ps]**	**DOI res FWHM [mm]**
DOI-capable	45	60	9.7 ± 0.4	**196 ± 6**	**146 ± 4**	**2.4 ± 0.2**
Standard	45	60	8.2 ± 0.2	**124 ± 3**	-	-

LYSO:Ce matrices 3.1x3.1x15 mm^3:

DOI- capable module:

Lateral irradiation:

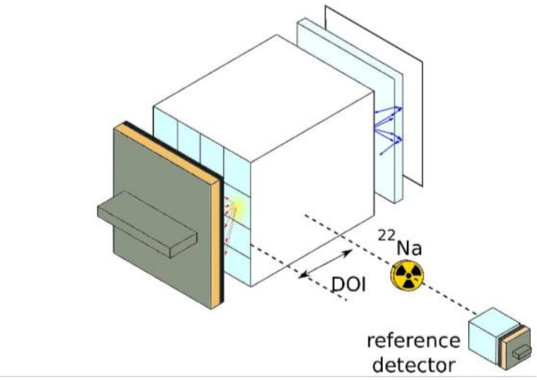

	Matrix type	V bias [V]	Thr. [mV]	En. Res FWHM [%]	**CTR std FWHM [ps]**	**CTR doi corr. FWHM [ps]**	**DOI res FWHM [mm]**
	DOI-capable	45	60	9.7 ± 0.4	**196 ± 6**	**146 ± 4**	**2.4 ± 0.2**
	Standard	45	60	8.2 ± 0.2	**124 ± 3**	-	-
PETsys*	DOI-capable				**291 ± 6**	**216 ± 6**	**2.6 ± 0.2**
PETsys*	Standard				**193 ± 6**	-	-

* *Measurements performed in collaboration with* RWTH *Aachen University*.
G. Terragni et al "Exploring the performance of a DOI-capable TOF-PET module using different readout electronics", article under preparation

Heterostructure concept:

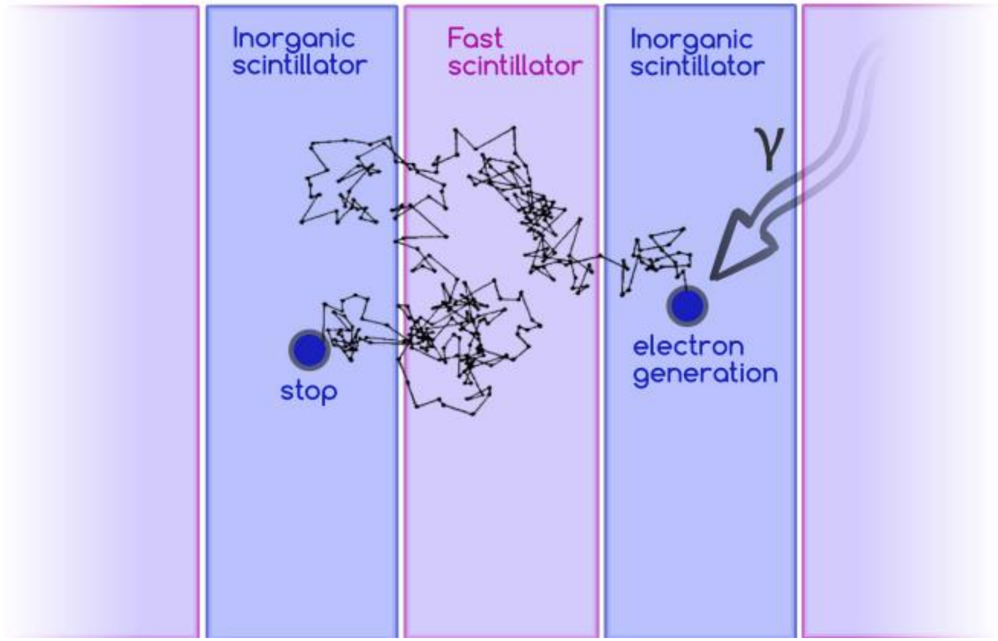

Energy sharing between inorganic and fast scintillator

- Combination of 2 materials with distinct properties (5 6 7)
- **Inorganic scintillator** like **BGO**: High stopping power for gamma rays at 511 keV
- **Fast scintillator** like **EJ232**: High photon density (large number of photons in the first ns)

(5) *ERC Advanced Grant TICAL (grant agreement No 338953, PI: P. Lecoq, CERN).*
(6) *R. Martinez Turtos et al 2019 Phys. Med. Biol. 64 and F. Pagano et al. Physics in Medicine & Biology, 2022, 67.13: 135010.*
(7) *F. Pagano et al. 2023 IEEE Transactions on Nuclear Science.*

Heterostructure matrices 3.1x3.1x20 mm^3:

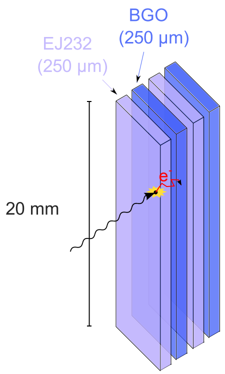

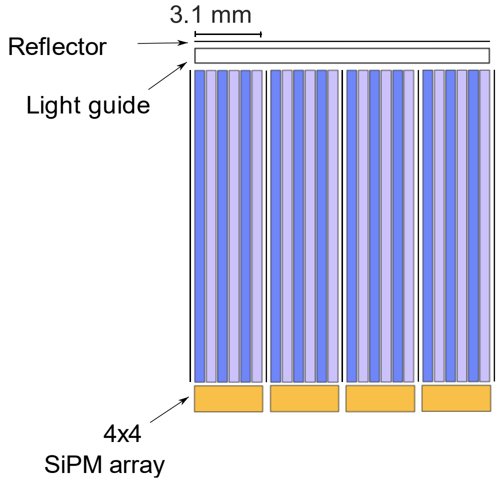

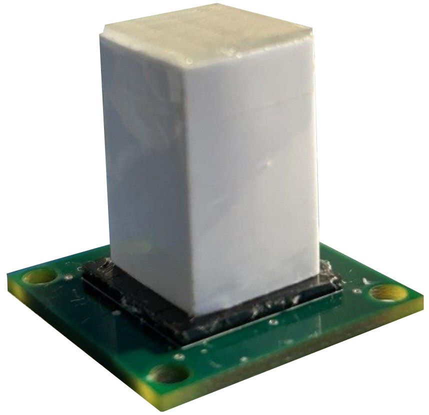

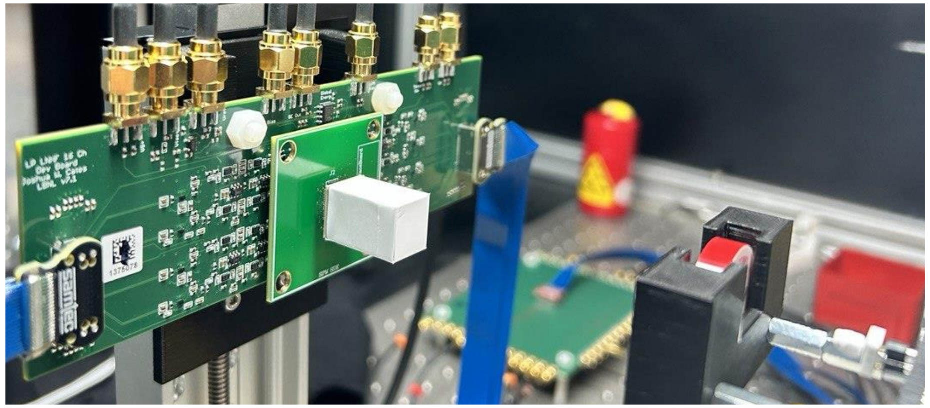

Heterostructure matrices 3.1x3.1x20 mm^3:

2D and 3D reconstruction of the interaction points

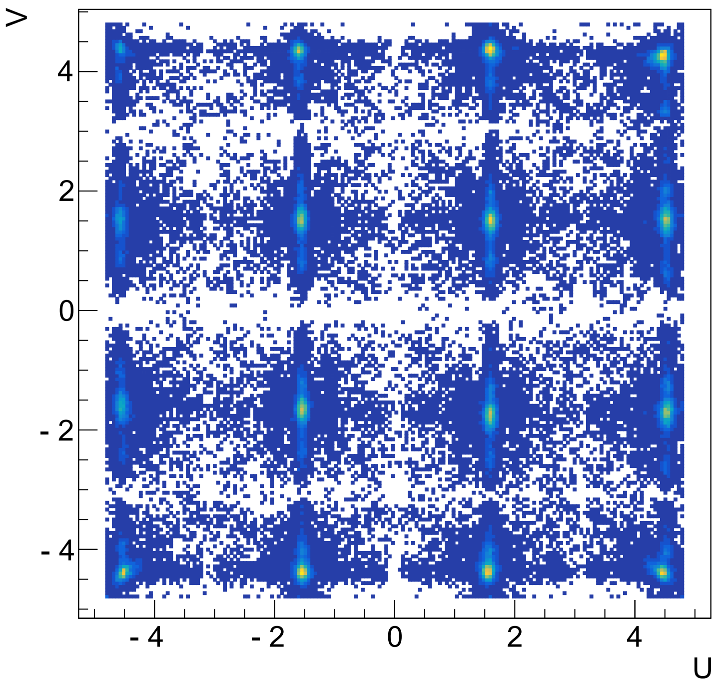

$$u = \frac{1}{P}\sum_{k=1}^{K} p_k x_k \ , \quad v = \frac{1}{P}\sum_{i=k}^{K} p_k y_k \ , \quad w = \frac{p_{max}}{P}$$

Energy sharing between BGO and EJ232

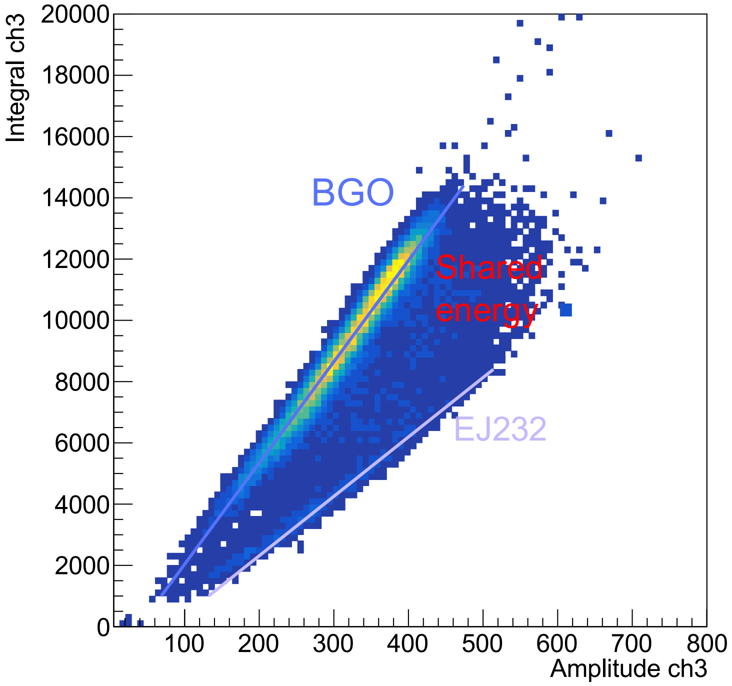

Observed for each pixel of the matrix

Heterostructure matrices 3.1x3.1x20 mm^3:

2D and 3D reconstruction of the interaction points

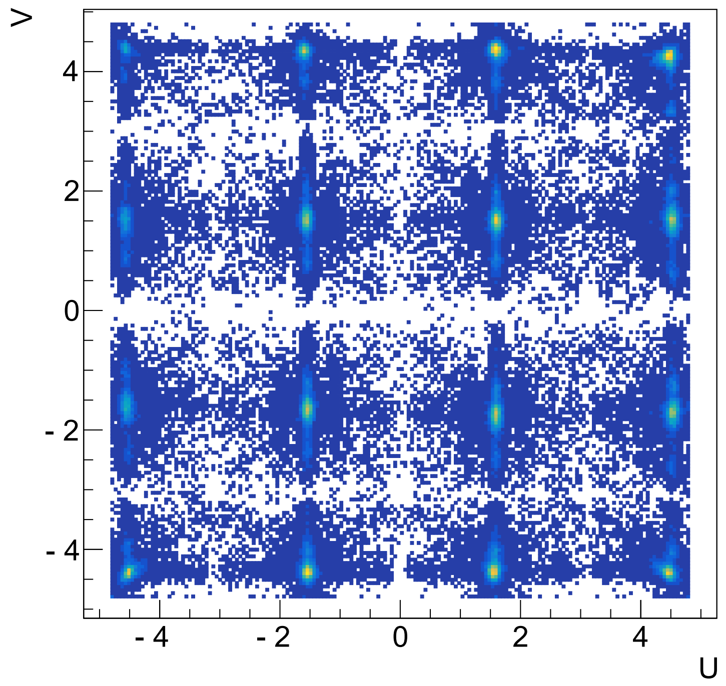

$$u = \frac{1}{P}\sum_{k=1}^{K} p_k x_k \ , \quad v = \frac{1}{P}\sum_{i=k}^{K} p_k y_k \ , \quad w = \frac{p_{max}}{P}$$

Energy sharing between BGO and EJ232

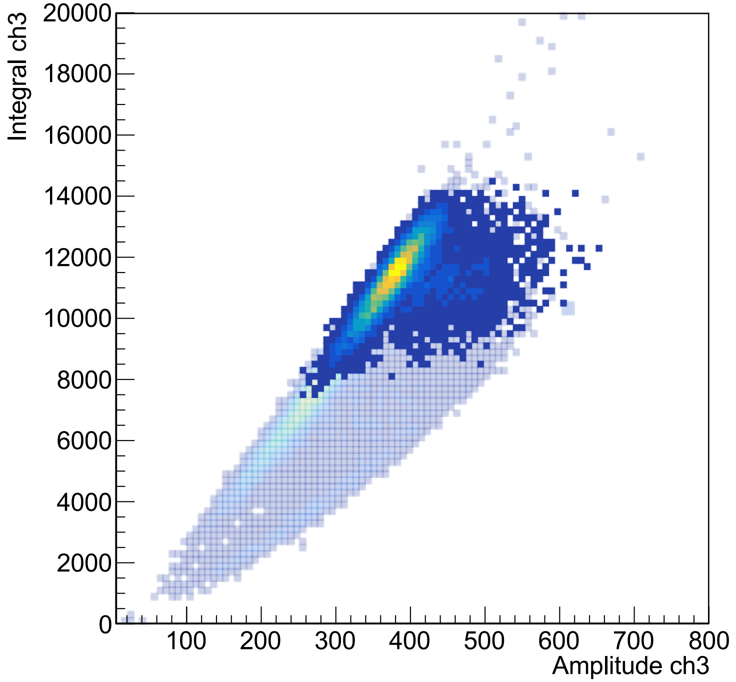

Observed for each pixel of the matrix

Heterostructure matrices 3.1x3.1x20 mm^3:

DOI- capable module:

Front irradiation:

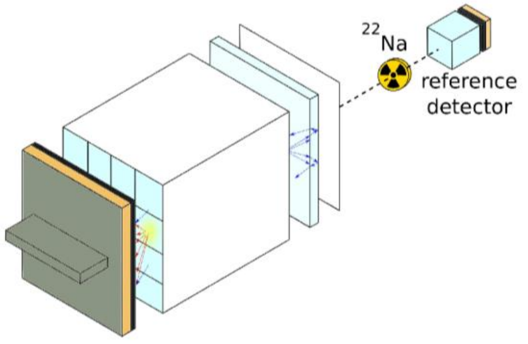

"All photopeak"

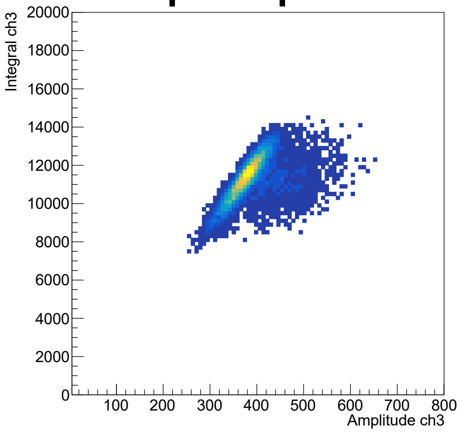

"Shared"

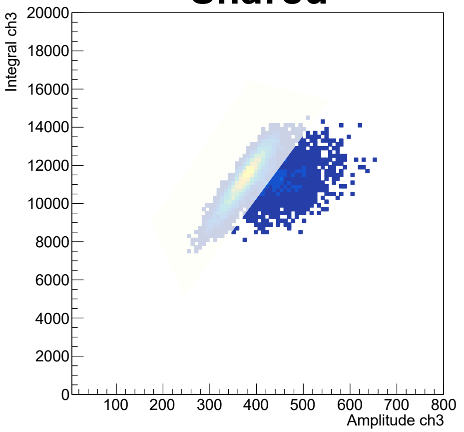

Events type	V bias [V]	Thr. [mV]	**CTR std FWHM [ps]**	**CTR doi corr. FWHM [ps]**
"All photopeak"	45	10	**290 ± 11**	**270 ± 9**
"Shared"	45	10	**194 ± 8**	**182 ± 6**

Preliminary !

Conclusions:

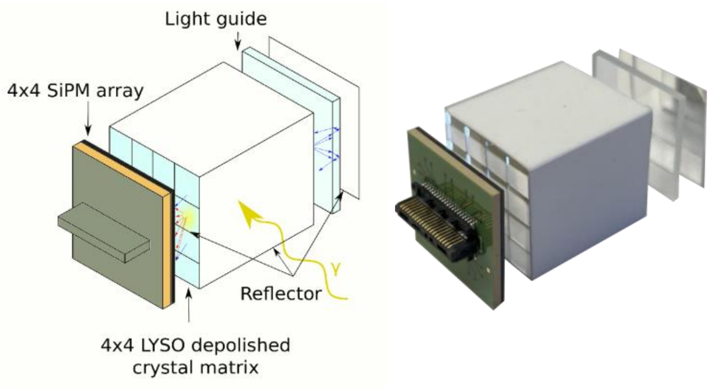

DOI-capable module

To enhance spatial, time and energy resolutions:

- Segmented detector 4x4 channels
- LYSO:Ce crystals
- Depolishing of the surface and light guide

$$u = \frac{1}{P}\sum_{k=1}^{K} p_k x_k \ , \quad v = \frac{1}{P}\sum_{i=k}^{K} p_k y_k \ , \quad w = \frac{p_{max}}{P}$$

Conclusions:

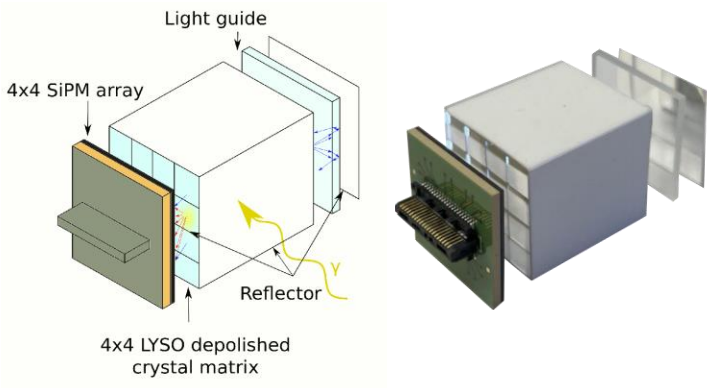

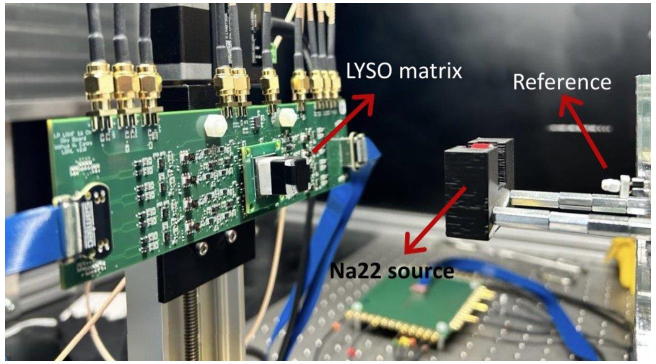

DOI-capable module

To enhance spatial, time and energy resolutions:

- Segmented detector 4x4 channels
- LYSO:Ce crystals
- Depolishing of the surface and light guide

$$u = \frac{1}{P}\sum_{k=1}^{K} p_k x_k \ , \quad v = \frac{1}{P}\sum_{i=k}^{K} p_k y_k \ , \quad w = \frac{p_{max}}{P}$$

Low-noise low-power high-frequency development board

To exploit the first photons produced and push the timing performance to the limit.

Using 4x4 3.1x3.1x15 mm^3 LYSO:Ce matrix and Broadcom MT SiPM array:

- Standard module: CTR = 124 ± 3 ps
- DOI-capable module: CTR = 146 ± 4 ps,
  DOI res = 2.4 ± 0.2 mm

Conclusions:

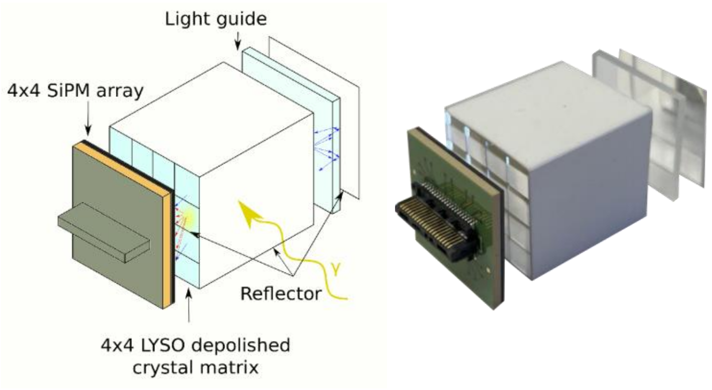

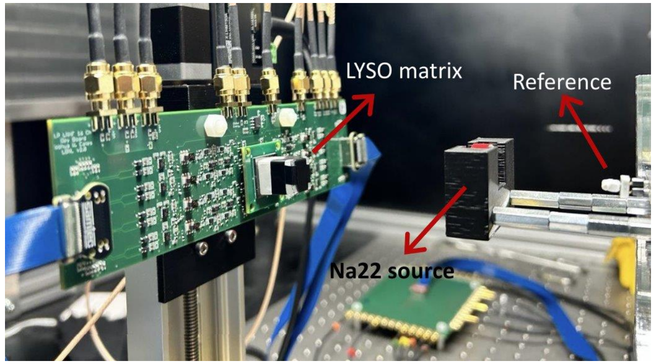

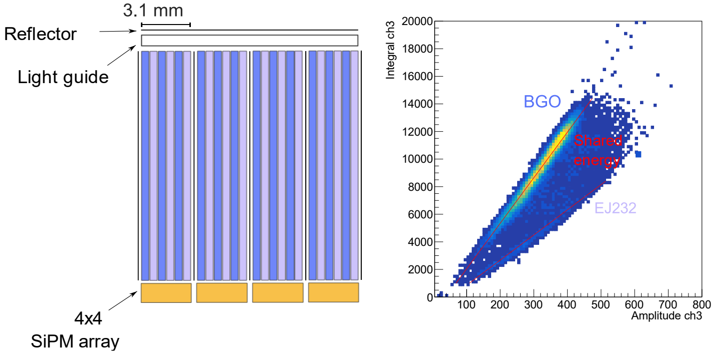

DOI-capable module

To enhance spatial, time and energy resolutions:

- Segmented detector 4x4 channels
- LYSO:Ce crystals
- Depolishing of the surface and light guide

$$u = \frac{1}{P}\sum_{k=1}^{K} p_k x_k \ , \quad v = \frac{1}{P}\sum_{i=k}^{K} p_k y_k \ , \quad w = \frac{p_{max}}{P}$$

Low-noise low-power high-frequency development board

To exploit the first photons produced and push the timing performance to the limit.

Using 4x4 3.1x3.1x15 mm^3 LYSO:Ce matrix and Broadcom MT SiPM array:

- Standard module: CTR = 124 ± 3 ps
- DOI-capable module: CTR = 146 ± 4 ps,
  DOI res = 2.4 ± 0.2 mm

Heterostructured scintillators

Alternating layers of two materials with complementary properties: high stopping power (BGO) and ultrafast timing (EJ232).

- Energy sharing between the two materials
- Impaired light transport due to the layered structure can be employed to retrieve the DOI information.

Outlooks:

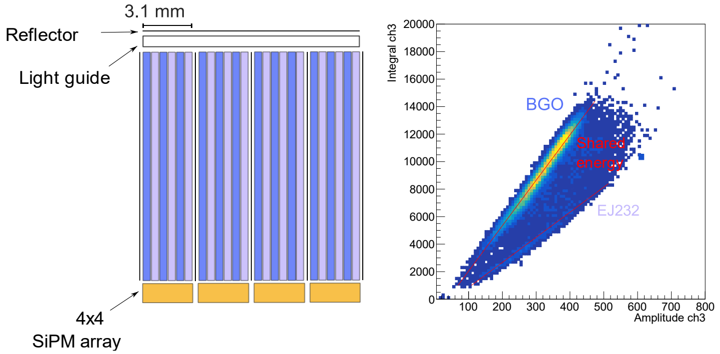

Heterostructured scintillators

Alternating layers of two materials with complemen tary properties: high stopping power (BGO) and ultrafast timing (EJ232).

- Energy sharing between the two materials
- Impaired light transport due to the layered structure can be employed to retrieve the DOI information .

Next steps:

Heterostructures:

- Evaluation of energy and DOI resolutions with front and lateral irradiation.
- Events classification for reconstruction.

Test of bulk materials:

- BGO matrices
- EJ232 matrices
- LYSO:Ce:Ca matrices

with different geometries and light guide compositions.

Acknowledgements

This work is carried out in the framework of the Crystal Clear Collaboration.

It received support from CERN Austrian and Gentner (grant no. 13E18CHA) Doctoral Programmes and CERN Budget for Knowledge Transfer to Medical Applications.

The development of the readout boards is supported by the National Institute of Biomedical Imaging and Bioengineering under award 5TR01EB028286.

E-mail:

giulia.terragni@cern.ch

Advancements in DOI-capable TOF-PET modules based on High-Frequency Readout

Giulia Terragni [1 2], Elena Tribbia [1 3], Carsten Lowis [1 4], Fiammetta Pagano [1 3 5],
Joshua W. Cates [6], Marco Pizzichemi [1 3], Johann Marton [2], Etiennette Auffray [1]

[1] CERN, Geneva, Switzerland. [2] Technical University of Vienna, Austria.
[3] University of Milano-Bicocca, Italy. [4] RWTH Aachen University, Germany.
[5] Institute of Instrumentation for Molecular Imaging (I3M), Valencia, Spain.
[6] Lawrence Berkeley National Laboratory, CA, USA.

28th May 2024
PM2024 - 16th Pisa Meeting on Advanced Detectors